INFLUENCES OF FRICTION STIR WELDING ON THE MICROSTRUCTURE, MECHANICAL AND CORROSION BEHAVIOUR OF AL-ZN-MG ALUMINIUM ALLOY 7039

C. Sharma[1*] – D. K. Dwivedi [2] – P. Kumar [3]

[1] Faculty of Mechanical Engineering, Rustamji Institute of Technology, Boarder Security Force Academy Tekanpur Gwalior, Madhya Pradesh, India-475005
[2, 3] Faculty of Mechanical Engineering, Indian Institute of Technology, Roorkee, Uttarkhand, India-247667

Abstract:

This paper presents the influence of friction stir welding (FSW) on the microstructure, mechanical and corrosion behavior of precipitation hardening Al-Zn-Mg alloy AA7039. The microstructure of weld joints was investigated using an optical microscope. The grains in weld nugget zone (WNZ) and thermo-mechanically affected zone (TMAZ) of weld joints were finer than in the base metal and a reverse trend was observed for heat affected zone (HAZ). Mechanical properties of friction stir weld joints were determined by tensile and micro hardness test. The ultimate tensile strength of weld joints was found approximately equal to the base metal while yield strength and ductility of weld joints were found lower than in the base metal. HAZ of weld joints was more susceptible to corrosion than WNZ, TMAZ and base metal. The HAZ exibits the highest current density followed by the base metal.

1 Introduction

Aluminum and its alloys are attractive construction materials for various engineering applications but the presence of natural oxide layer, solute elements and higher solubility of hydrogen imposes great difficulties in fusion welding of most of the aluminum alloys, especially 2xxx and 7xxx series precipitation hardening alloys [1, 2]. Alternatively, these can be joined successfully by friction stir welding (FSW), a solid-state hot-shear joining process which was invented at the Welding Institute (TWI), Cambridge UK in 1991.
In FSW, a non consumable rotating tool with a shoulder and threaded pin is lowered until shoulder makes firm contact with the top surface of the work-piece. The rotating tool then traverses along the butting surfaces of two rigidly clamped plates placed on a backing plate. The heat is produced by the friction between the tool and the material being joined and to a lesser extent at the pin work piece interface, which causes the weld material to soften around the pin at a temperature less than its melting point [3, 4]. The softened material underneath the shoulder is subjected to extrusion by rotary and traverse movement of the tool; it is transported from the advancing side to the retreating side where it is consolidated into a joint [5]. The joint is formed by dual action of extrusion and forging at temperatures

---

* Corresponding author. Tel.: +91-1332-285826, Fax: 91-1332 -285665
 E-mail address: chaitanya.sharmaji@gmail.com

below the melting point temperature of material being joined. Therefore, melting and solidification is absent in the friction stir weld joint avoiding thus most of the problems of fusion welding of aluminium alloys [3, 4]. Moreover, FSW joints offer many attractive advantages over fusion welding such as superior joint properties and fatigue lives, low energy consumption, no harmful emission and therefore, they are increasingly preferred for joining aluminum alloys for rail, marine, automotive and aerospace applications [3, 4].

Literature review revealed that considerable work has been reported on various aspects of friction stir welded precipitation hardening (2XXX, 6XXX and 7XXX series) aluminum alloys such as material flow, the development of microstructure and mechanical properties, the effect of process parameters, in-process cooling, post weld heat treatment, fatigue and corrosion behavior [5-10]. However, limited work [11-19] is available on friction stir welding of Al-Zn-Mg alloy 7039. This alloy is used in military and other light weight structural applications like transportable bridges, girders, armor plates, bumpers, cryogenic pressure vessels where on site repair and maintenance work is required [12, 13]. In view of wide spread applications of these alloys, in this work, an attempt has been made to friction stir weld Al-Zn-Mg alloy 7039 in order to investigate the influence of friction stir welding on the microstructure, mechanical and corrosion behavior of Al-Zn-Mg aluminium alloy 7039.

2   Material and experimental procedures

Five millimeter thick extruded plates of Al-Zn-Mg alloy 7039-O were used as the base metal for this experimental investigation. The chemical composition and mechanical properties of the base metal are presented in Table 1 and 2, respectively.

A vertical milling machine (HMT India, 5 KW, and 635 rpm) was modified for FSW. For this, the machine was equipped with indigenously designed fixture and collates to hold base metal plates and tool in desired position during FSW. In another study [13], authors have investigated the effect of process parameters on the microstructure and mechanical properties of FSW joints of 7039 aluminum alloy. It was found that mechanical properties are increased by either decreasing welding speed or increasing rotary speed. The FSW joints were produced by welding at the speed of 75 mm/min and rotary speed of 635 rpm exhibited maximum mechanical

properties. The optimum combination of welding and tool geometry parameters similar to previous study [13] is used in this work for the production of FSW joints. Tool used for FSW was fabricated using die steel, and had flat shoulder with truncated conical pin. The pin had anticlockwise thread of 1 mm pitch. These tools were heat treated to increase their hardness prior to use.

Table 1. Chemical composition of base metal

Chemical composition (Wt %)						
Zn	Mg	Mn	Fe	Si	Cu	Al
4.69	2.31	0.68	0.69	0.31	0.05	Rem.

Table 2. Mechanical properties of base metal

Mechanical Properties			
Ultimate Tensile Strength (MPa)	Yield Strength (MPa)	Elongation (%)	Micro Hardness (Hv)
212.7	88.9	38.4	65

After FSW, the quality of developed joints was assessed by three point bend test to reveal the presence of subsurface defects. All weld joints passed the bend tests and no crack was observed on the external surfaces subjected to bending. Tensile tests specimens were prepared using ASTM E8M guidelines and tested on computerized UTM (H25K-S, Hounsfield), using a crosshead speed of 1 mm/min. The machine was equipped with Q Mat software (Version 5.35) to record load and extension data during test so as to perform post test analysis. Three tensile tests were performed in each condition and average values were used for discussion.

A Vickers microhardness tester (VHM-002V Walter UHL, Germany) was used for measuring the variation of hardness across the weld joints. Indentation for microhardness measurements were made with a load of 1 N for 30 s dwell time at the mid-thickness on the samples taken from transverse direction of the FSW joints. In general, the spacing between two consecutive indentations should be more than 2-5 times the diagonal of the indentation. After FSW, samples for metallographic investigation were extracted from the weld joint using a bend saw.

Subsequently, samples were mounted in self curing commercially available resin 'Bond tite'. Mounted samples were then polished up to 1200 grade-SiC paper finish and then cloth polishing was done using 1 μm alumina suspensions on disk polisher. Polished samples were etched in Keller's reagent (2 ml nitric acid, 4 ml hydrofluoric acid and 94 ml water) for 90 s for macro and microstructural observation. The microstructure of FSW joints etched in Keller's reagent was observed using a light optical microscope (Leica, Germany) and grain sizes of α Al were determined using Image J, image analysis software. The fracture surfaces of the tensile tested specimens were investigated by a FE-SEM (FEI-Quanta 200 ®).

Prior to immersion corrosion test, the specimens were grounded to 1200 grit SiC paper finish, cleaned with ultra-sonic cleaner using distilled water as a medium and dried in air. A flat corrosion cell was used with three electrodes, test sample of 0.5 cm² exposed area, Ag/AgCl saturated KCl reference electrode and platinum wired counter-electrode. Scan rates were applied to the cell with the use of PARSTAT 2273®, operated by PowerSuite® software. The surface roughness values, before and after immersion in 3.5% NaCl solution, is measured by a Wyko NT 1100 optical profilometer interfaced with Vision®32 software.

3 Results

3.1 Macrostructure

FSW joints exhibited WNZ, TMAZ and HAZ surrounded by the base metal, as shown in Fig. 1. From the optical micrographs it is evident that FSW changed the starting microstructure of the base metal more than in the WNZ, TMAZ and HAZ. The base metal had equiaxed grain structure of an average size of 27.6 μm with uniformly distributed strengthening precipitates (Fig. 1 (a)). WNZ showed dynamically recrystallized equiaxed grains of an average size of 6.4 μm (Fig. 1 (b)). Next to WNZ is the TMAZ where grains were deformed bent and elongated in upward flow pattern. The average size of deformed grains in TMAZ was 15.3 μm. HAZ exhibited a microstructure similar to the base metal but grains were significantly coarser than the base metal. The average size of coarse grains was 38.3 μm. The extent of grain refinement is found to decrease from the central WNZ to the outermost HAZ. Grains in WNZ and TMAZ were approximately 4.3 and 1.8 times finer

than of the base metal (27.6 μm), while grains in HAZ were 1.4 times coarser than of the base metal. Moreover, TMAZ and HAZ showed strengthening precipitates while the same were not observed in the WNZ (Fig. 1 (b)).
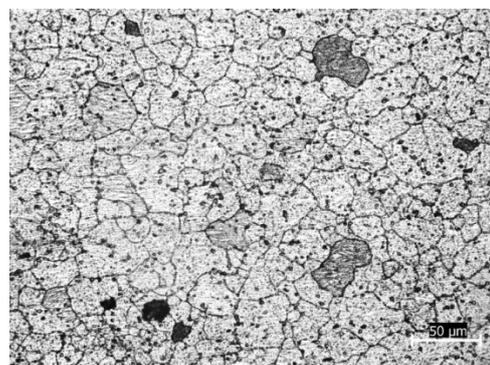
a)
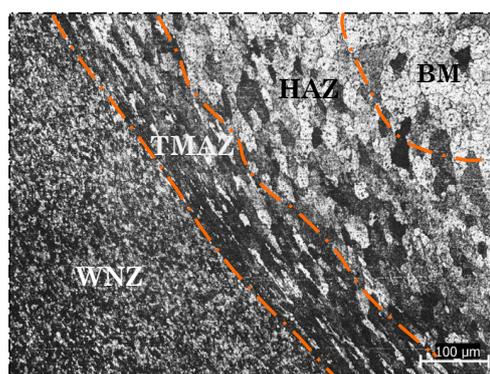
b)

Figure 1. Microstructure of (a) base metal (b) FSW joints showing WNZ, TMAZ and HAZ.

3.2 Mechanical properties

3.2.1 Microhardness

The mid plane transverse microhardness profile of FSW joints along with base metal is shown in Fig. 2. From microhardness profile it is evident that FSW strengthens the weld joint resulting in significantly higher microhardness of FSW joint than the base metal. The average microhardness of WNZ and HAZ of FSW joints was approximately 104 Hv, which was significantly higher than the microhardness of the base metal (65 Hv). Microhardness profile is asymmetric; the grain size in microhardness is decreased from WNZ to base metal. Minimum

microhardness was recorded in the base metal on retreating side.
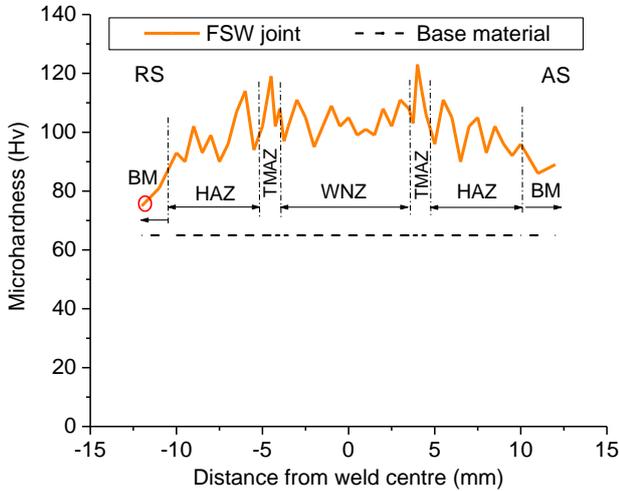
Figure 2. Microhardness variations across the FSW joint.

3.2.2 Tensile properties

Fig. 3 shows the strain-stress diagram for FSW joints and base metal. From strain-stress diagram it is evident that tensile strength of FSW joints is approximately similar to the base metal while % elongation is significantly lower than the base metal. The ultimate tensile strength, yield strength and % elongation of FSW joints were 208.9 MPa, 88.9 MPa and 23.6%, respectively, while those of base metal were 212.7 MPa, 105.6 MPa and 38.4 %. The ratio of tensile property of FSW joints to that of base metal is defined as the joint efficiency.
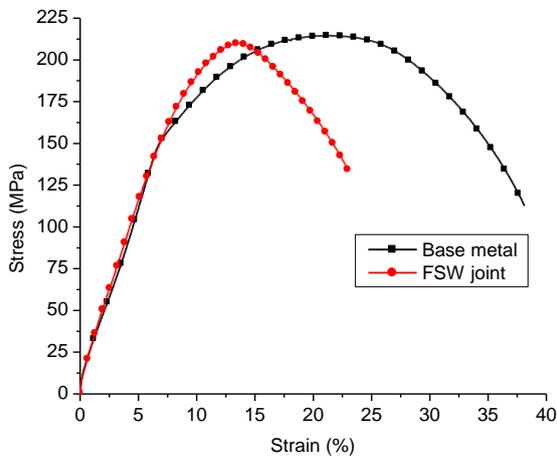
Figure 3. Strain-stress diagram for FSW joint and base metal.

Accordingly, the tensile strength efficiency, yield strength efficiency and elongation efficiency of FSW joints were 98.2%, 84.2% and 61.5%, respectively. The analysis of results suggests that FSW had more pronounced influence on % elongation than tensile strength of FSW joints.

During transverse tensile test, FSW joints fractured from minimum microhardness region of base metal on the retreating side. Fracture morphology was ductile for the base metal and FSW joints as evident from dimpled fracture surfaces shown in Fig. 4. Fracture surfaces of FSW joints were coarser grained than the base metal.
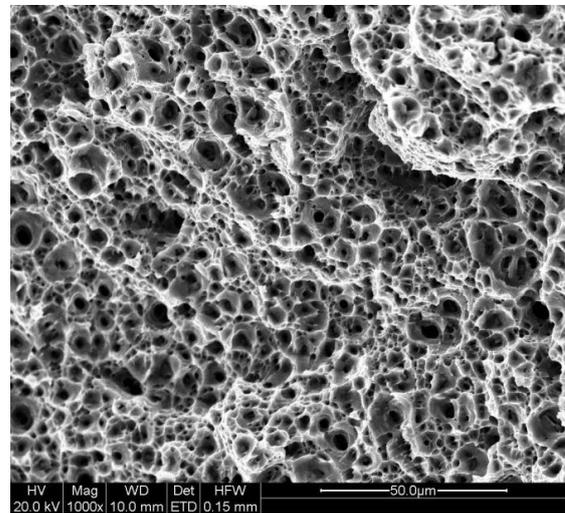
a)
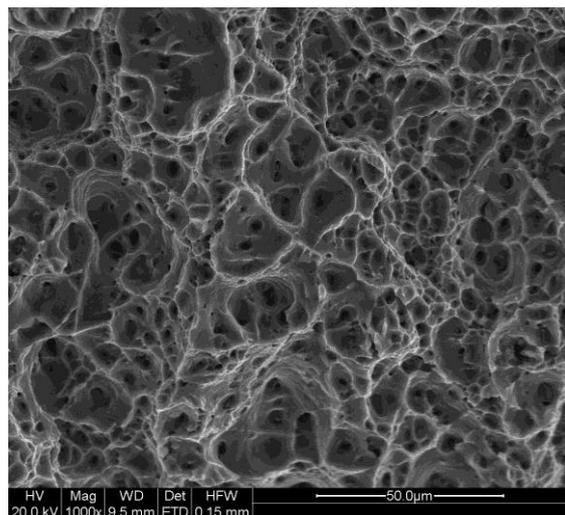
b)

Figure 4. Fracture surfaces, (a) Base metal, and (b) FSW joint of AA7039.

_____

The breakage of secondary precipitates rich in Mg and Zn triggered the formation of micro voids at grain boundary particles whose coalescence resulted in fracture of FSW joints. Cavaliere et al. [20] observed similar failure pattern for AA 6082 FSW joints.

The ductile behavior of the material before failure was revealed by a larger population of very fine dimples while a less ductile behavior was revealed by the presence of a minor population of voids larger in size on the fractured surface of joints.

3.3 Corosion behavior

The corrosion potential (E_{corr}) is a unique mixed potential whose rates of anodic and cathodic reaction are exactly the same and equal the corrosion rate [21]. Potentiodynamic polarization curves for Tafel analysis (in 3.5% NaCl solution) of base metal, WNZ, TMAZ and HAZs of FSW joints are shown in Fig. 5.
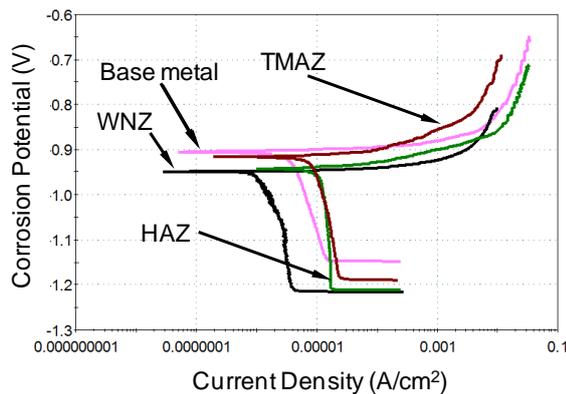
Figure 5. Potentiodynamic polarization curves for Tafel analysis in 3.5% NaCl solution.

Surprisingly, all potentiodynamic polarization curves exhibited similar shape, showing first a cathodic plateau related to the oxygen reduction related reaction. The cathodic current density was found in the range of 10^{-6} - 10^{-4} A/cm^2 for different zones of FSW joints and base (Fig. 5). Only one breakdown potential corresponding to OCP was observed as evident from polarization curves. All the samples were suceptible to corrosion in 3.5% NaCl solution as no passivation plateu was observed. Anodic branch of the Tafel curve initially exhibited a rapid and strong increase in anodic current density with a slight increase in corrosion potential. Afterwards, anodic current density was slowly increased with a prompt increase in corrosion potential. The HAZ exhibited highest current density, approximately 9.1

µA /cm^2 while WNZ showed the lowest current density, approximately 1.3 µA /cm$^{2.}$ The current density of HAZ was found to be ~3.5-7 times higher than the base metal, WNZ and TMAZ resulting in severe corrosion of the same. Except for HAZ, FSW weld joint showed lower current density than the base metal, suggesting thus better corrosion resistance. These results suggest that WNZ and TMAZ had better corrosion behavior than the base metal, while HAZ showed poorer corrosion behavior than the base metal.

Images of corroded surfaces of the base metal and different zones of FSW joints after immersion corrosion test in 3.5% NaCl solution are shown in Fig. 6. The base metal showed many tiny and small pits while WNZ exhibited few pits (black in color). TMAZ exhibits somewhat larger pits than base metal and WNZ. The HAZ of FSW joints showed long and wide grooves. Average surface roughness of all corroded specimens was higher (150.3-590.4 nm) than un-corroded specimen (92.1 nm).

a)

b)
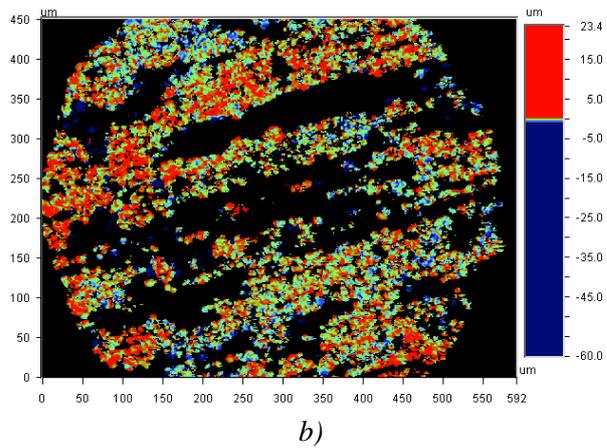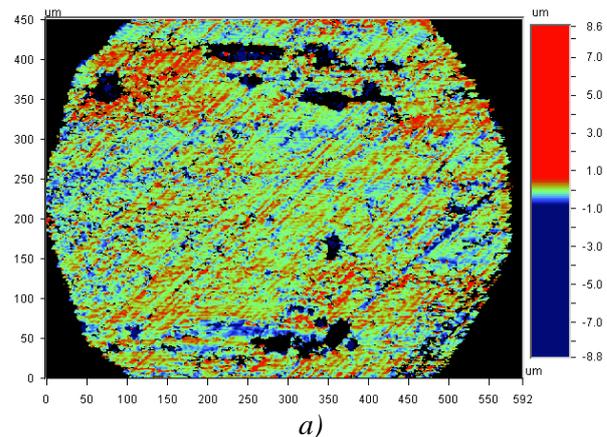
Figure 6. Corrosion surface: (a) WNZ, and (b) HAZ of friction stir weld joint of AA7039-O.

The HAZ resulted in the highest surface roughness (590.4 nm) and WNZ in the lowest surface roughness (150.3 nm). These results are in accordance with results obtained from Tafel analysis which showed higher current density i.e., corrosion rate for HAZ and consequently poorer surface finish of the same. Base metal showed many tiny and small pits while WNZ exhibited few pits (black in color). TMAZ exhibits somewhat larger pits than base metal and WNZ. The HAZ of FSW joints showed long and wide grooves. Average surface roughness of all corroded specimens was higher (150.3-590.4 nm) than un-corroded specimen (92.1 nm). The HAZ resulted in the highest surface roughness (590.4 nm) and WNZ in lowest surface roughness (150.3 nm). These results are in accordance with the results obtained from Tafel analysis which showed higher current density i.e., corrosion rate for HAZ and consequently poor surface finish of the same.

4   Discussion

Based on the results of this study, it can be noted that friction stir welding had paramount influence on the microstructure, mechanical and corrosion behavior of FSW joints. FSW joints showed dynamically recrystallized, deformed and coarser grains in WNZ, TMAZ and HAZ, respectively than coarse equiaxed grains of the base metal. Grains in WNZ and TMAZ were approximately 4.3 and 1.8 times finer than the base metal (27.6 μm). While grains in HAZ were 1.4 times coarser than the base metal. WNZ is the region just beneath the tool shoulder and is subjected to severe combination of thermo mechanical stresses generating high temperature ~ 480°C which in turn cause dynamic recrystallization [6 -8]. Thus coarse grain structure of base material transforms into fine and equiaxed grain structure in WNZs. As compared to the base material, fewer second phase strengthening precipitates of MgZn$_2$ were observed in WNZs as these are dissolved/ broken down and uniformly distributed by stirring tool [12-14]. TMAZ lying at the edge of tool shoulder exhibits bent and elongated non recrystallized grains due to shearing by rotating tool. The HAZ is the outermost region influenced by thermal transient only. The temperatures (250-350 °C) attained in HAZ are sufficient to cause static grain growth which in turn coarsens grains in HAZ [7].

The average microhardness of FSW joints was higher than the base metal while mechanical properties of FSW joints were comparable to the base metal.

Solution strengthening and strain hardening effect due to severe plastic deformation resulted in significantly higher microhardness of WNZ of FSW joints than base metal. While post-weld artificial aging of previously solutionized base metal resulted in higher microhardness of HAZ than the base metal. FSW joints showed lower % elongation than the base metal despite recrystallized grain structure in WNZ. The decrease in elongation of FSW joints can be attributed to two important factors. Firstly, strengthening of weld joints and the presence of coarser second phase strengthening precipitates in HAZ reduces elongation (it seems hardening dominates over recrystallization). Secondly, confined flowability of material due to strain localization in the weakest zone, during transverse tensile test may also reduce overall ductility of weld joints.

FSW joints fractured from base metal on retreating side. Similar results were reported by Threadgil et al. [3] and Sharma et al. [19] for aluminum alloys friction stir welded in annealed condition. Failure of cross weld joint during tensile test can occur anywhere on the specimen but it usually occurs in the base metal away from the weld.

All the samples were suceptible to corrosion in 3.5% NaCl solution as no passivation plateu was observed [22]. WNZ and TMAZ of FSW joints have better corrosion resistance than the base metal while reverse trend was observed for HAZ. The current density for HAZ was ~3.5-7 times higher than the other resulting in higher corrosion rates. The main strengthening precipitate in Al-Zn-Mg alloy AA7039 is MgZn$_2$ [8, 13-15]. The η phase strengthening precipitates are found both in α aluminum matrix and at grain boundaries. These η pahse precipitates were dissolved in WNZ and coarsened at grain boundary in FSW joint depending upon FSW parameters [2]. The WNZ had refined grain structure and more uniform pecipitate distribution than the base metal which in turn results in better corrosion behavior of the same. The grain structure in HAZ is simillar to the base metal except for coarse precipitates. Further chances of formation of precipitates free zone (PFZs) along subgrain boundaries exist more in HAZ due to senitization. Senitization (owing to thermal effects) leads to the depletion of Zn and formation of solute free zones [23, 24]. These precipitates free zones (PFZs) are found to be more reactive than α aluminum matrix resulting in slightly greater anodic reactivity of HAZ than in base metal and other zones of FSW joints, thus making HAZ more sucesspetible to corrosion [22-24].

5 Conclusions

Friction stir welding of Al-Zn-Mg alloy AA7039 is recommended to be performed in O temper condition because developed FSW joints exhibited higher tensile strength and better corrosion resistance possibly due to more uniform distribution of fine MgZn$_2$ precipitates in affected zone than in the base metal. Friction stir welding strengthens the WNZ and HAZ of FSW joints and therefore mechanical properties of FSW joints were comparable to the base metal. Fracture location was located in the base metal i.e., away from FSW joints. WNZ and TMAZ of FSW joints have better corrosion resistance than the base metal. Higher corrosion rates make HAZ more suceptible to corrosion than base metal.

References

[1] Cam, G., Kocak, M.: *Microstructural and mechanical characterization of electron beam welded Al-alloy 7020*, Journal of Material Science, 42 (2007), 7154–7161.

[2] Hassan, Kh. AA., Prangnell, P.B., Norman, A.F., Price, D.A., Williams, S.W.: *Effect of welding parameters on nugget zone microstructure and properties in high strength aluminium alloy friction stir welds*, Science and Technology of Welding and Joining, 8 (2003), 4, 257–268.

[3] Threadgill, P. L., Leonard, A. J., Shercliff, H. R., Withers, P. J.: *Friction stir welding of aluminium alloys*, International Materials Reviews, 54 (2009), 2, 49-93.

[4] Mishra, R.S., Ma, Z. Y.: Friction stir welding and processing, Material science engineering R, 50 (2005), 1–78.

[5] Colligan, K.: *Material flow behaviour during friction welding of aluminum*. Welding Journal, (1999), pp. 229-237.

[6] Ji S., Jin Y., Yue Y., Zhang L., Lv Z.: *The effect of tool geometry on material flow Behavior of friction stir welding of titanium Alloy*. Engineering Review, 33 (2013), 2, 107-113.

[7] Mahoney, M.W., Rhodes, C.G., Flintoff, J.G., Spurling, R.A, Bingel, W.H.: *Properties of FSWed 7075 T651 Al*, Metallurgical & Materials Transactions, A 29 (1998), 1955-1964.

[8] Jata, K.V., Sankaran, K.K., Ruschau, J.: *Friction stir welding effects on microstructure and fatigue of aluminum alloy 7050-T7451*, Metallurgical and Materials Transactions, A 31, (2000), 2181–2192.

[9] Liu, H.J., Chen, Y.C., Feng, J.C.: *Effect of heat treatment on tensile properties of FSWed joints of 2219-T6 Al alloy"*, Material Science and Technology, 22, (2006), 2, 237–241.

[10] Xu, W., Liu, J.: *"Microstructure and pitting corrosion of FSWed joints in 2219-O aluminum alloy thick plate"*, Corrosion Science, 51 (2009) 2743–2751.

[11] Balasubbramanian, V. *"Relationship between base metal properties and FSW process parameters"*, Materials science and engineering A, 480 (2008), 397-403.

[12] Singh, R.K.R., Chaitanya Sharma, Dwivedi, D.K., Mehta, N.K, Kumar, P.: *The microstructure and mechanical properties of friction stir welded Al–Zn–Mg alloy in as welded and heat-treated conditions*. Materials & Design, 32 (2011), 682-687.

[13] Sharma C., Dwivedi, D. K., Kumar, P.: *Effect of welding parameters on microstructure and mechanical properties of friction stir welded joints of AA7039 aluminum alloy*. Materials Design, 36 (2012), 379-390.

[14] Sharma, C., Dwivedi, D. K., Kumar, P.: *Influence of in-process cooling on tensile behavior of friction stir welded joints of AA7039*. Material Science & Engineering A, 556 (2012), 479-487.

[15] Chaitanya, S., Dheerendra, K. D., Pradeep, K.: *Friction stir welding of Al- Zn- Mg alloy AA7039*. TMS 141 annual meeting, Light Metals, Aluminum Alloys: Fabrication, Characterization and Applications. Orlando, Florida, USA, March, 2012, 503-507.

[16] Sharma, C., Dwivedi, D. K., Kumar, P.: *Effect of post weld heat treatments on microstructure and tensile properties of friction stir welded joints of Al-Zn-Mg alloy AA7039*. Materials and Design, 43 (2013), 134-143.

[17] Chaitanya, S., Dheerendra K. D., Pradeep, K.: *Corrosion behaviour of friction stir welded joints of Al-Zn-Mg alloy.* 2nd International Conference on Manufacturing Excellence (MANFEX 2013), Amity School of Engineering & Technology, Amity University, Noida (U.P), India, 2013, 157-161.

[18] Chaitanya, S., Dheerendra, K. D., Pradeep, K.: *Heterogeneity of microstructure and mechanical properties of friction stir welded joints of Al-Zn-Mg alloy AA7039*. Procedia Engineering, 64 (2013), 1384-1394.

[19] Chaitanya, S., Dheerendra, Kumar, D., Pradeep, K.: *Fatigue Behaviour of Friction Stir Weld Joints of Al-Zn-Mg alloy AA7039 Developed Using Base Metal in Different Temper Condition,* Materials & Design, 64 (2014), 334-344.

[20] Cavaliere, P., Squillace, A., Panella, F.: *Effect of welding parameters on mechanical and microstructural properties of AA6082 joints produced by friction stir welding*, Materials & Design, 30 (2009), 3, 609–616.

[21] ASM Handbook Volume 13A, *Corrosion: Fundamentals, Testing, and Protection.* ASM international material park, USA.

[22] Venugopal, T., Rao, K.S., Rao, K.P.: *"Studies on FSWed 7075 al alloy"*, Transactions of the Indian Institute of Metals, 57 (2004), 6, 659-663.

[23] Paglia, C. S., Buchheit, R. G.*: "A look in the corrosion of Al alloy FS welds"*, Scripta Materialia, 58 (2008), 383–38.

[24] Pao, P. S., Gill, S.J., Feng, C.R., Sankaran, K. K.: *Corrosion fatigue crack growth in FSWed 7050 Al alloy.* Scripta Materialia, 45 (2001), 605-612.